

Reconciling the local void with the CMB

Seshadri Nadathur and Subir Sarkar

Rudolf Peierls Centre for Theoretical Physics, University of Oxford, Oxford OX1 3NP, UK

(Dated: August 13, 2018)

In the standard cosmological model, the dimming of distant Type Ia supernovae is explained by invoking the existence of repulsive ‘dark energy’ which is causing the Hubble expansion to accelerate. However this may be an artifact of interpreting the data in an (oversimplified) homogeneous model universe. In the simplest inhomogeneous model which fits the SNe Ia Hubble diagram *without* dark energy, we are located close to the centre of a void modelled by a Lemaître-Tolman-Bondi metric. It has been claimed that such models cannot fit the CMB and other cosmological data. This is, however, based on the *assumption* of a scale-free spectrum for the primordial density perturbation. An alternative physically motivated form for the spectrum enables a good fit to both SNe Ia (Constitution/Union2) and CMB (WMAP 7-yr) data, and to the locally measured Hubble parameter. Constraints from baryon acoustic oscillations and primordial nucleosynthesis are also satisfied.

PACS numbers: 98.80.Es, 98.65.Dx, 98.62.Sb

I. INTRODUCTION

The simplest cosmological model consistent with the spatial flatness expectation of inflation is the Einstein-de Sitter (EdS) universe with $\Omega_m = 1$ and $\Omega_K = 0$. This formed the basis of the “standard cold dark matter” (SCDM) cosmology which provided a good description of the large-scale structure of the universe [1, 2]. It was noted however that it is inconsistent with the angular power spectrum of the clustering of galaxies in the APM survey [3]. Subsequently large-angle anisotropies in the cosmic microwave background (CMB) were detected by COBE [4], thus providing an absolute normalization of the amplitude of primordial density perturbations. The SCDM model assumes that the power spectrum of the primordial density perturbations has the scale-invariant form: $P(k) \equiv |\delta_k|^2 \propto k^n$, with $n = 1$ and the predicted amplitude of matter fluctuations on small (cluster and galaxy) scales is then too high relative to observations [5]. However if the epoch of matter-radiation equality is delayed by lowering the CDM density to $\Omega_m \sim 0.3$, then the peak in the power spectrum of density fluctuations is shifted to larger scales thus decreasing the power on small scales and enabling a match to the data. To maintain spatial flatness a non-zero value of the cosmological constant was invoked, with $\Lambda \sim 2H_0^2$ corresponding to $\Omega_\Lambda \equiv \Lambda/3H_0^2 \sim 0.7$. Subsequently it was also observed that Type Ia supernovae (SNe Ia) at redshift $z \simeq 0.5$ appear $\sim 25\%$ fainter than expected in an EdS universe [6, 7]. Together with measurements of galaxy clustering in the 2dF survey [8] and of cosmic microwave background (CMB) anisotropies by WMAP [9], this changed the standard cosmological model to an accelerating universe with a dominant cosmological constant term, which has been widely interpreted as a manifestation of the physical vacuum or “dark energy”. This “concordance” Λ CDM cosmology (with $\Omega_\Lambda \simeq 0.7$, $\Omega_m \simeq 0.3$, $h \simeq 0.7$) has proved to be consistent with other cosmological data, in particular, baryonic acoustic oscillations detected in the SDSS [10] and measurements of mass fluctuations

from clusters and weak lensing [11]. Further observations of both SNe Ia [12–14] and the WMAP 3-year results [15] have continued to firm up the model.

Embarrassingly, however, this model lacks a *physical* basis. There are two serious problems with the notion that the universe is dominated by some form of vacuum energy. The first is the notorious fine-tuning problem of vacuum fluctuations in quantum field theory — the energy scale of the inferred cosmological energy density is $\sim 10^{-12}$ GeV, which is many orders of magnitude below the energy scale of $\sim 10^2$ GeV of the Standard Model of particle physics, not to mention the Planck scale of $M_P \equiv (8\pi G_N)^{-1/2} \simeq 2.4 \times 10^{18}$ GeV [16]. The second is the equally acute coincidence problem: since Ω_Λ/Ω_m evolves as the cube of the cosmic scale factor $a(t)$, there is no reason to expect it to be of $\mathcal{O}(1)$ *today*, yet this is supposedly the case.

Interestingly the WMAP results alone do not require dark energy if the assumption of a scale-invariant primordial power spectrum is relaxed. This is well justified given our present ignorance of the physics underlying inflation which is believed to have created these fluctuations. It has been demonstrated [17, 18] that the temperature angular power spectrum of an EdS universe with $h \simeq 0.44$ matches the WMAP data well if the primordial power is enhanced by $\sim 30\%$ in the region of the second and third acoustic peaks (corresponding to spatial scales of $k \sim 0.01 - 0.1 h \text{ Mpc}^{-1}$). This alternative model with *no* dark energy has a slightly better χ^2 for the fit to WMAP-3 data than the concordance “power-law Λ CDM model” and, in spite of having more parameters, has an *equal* value of the Akaike information criterion used in model selection. Other EdS models with a broken power-law spectrum [19] have also been shown to fit the WMAP data. Moreover, an EdS universe can fit measurements of the galaxy power spectrum if it includes a $\sim 10\%$ component of hot dark matter in the form of massive neutrinos of mass ~ 0.5 eV [17–19]. Clearly the main evidence for dark energy comes from the SNe Ia Hubble diagram.

It should be kept in mind that the acceleration of the

expansion rate is not directly measured but inferred from measurements of the apparent magnitudes and redshifts of SNe Ia. Indeed *all* the evidence for dark energy is geometrical, i.e., based on interpreting the data in an assumed homogeneous model universe. So far there is no convincing observation of dynamical manifestations, e.g., the “late integrated Sachs-Wolfe effect”. In fact what is actually inferred from observations is *not* an energy density, just a value of $\mathcal{O}(H_0^2)$ for the otherwise unconstrained Λ term in the Friedmann equation. It has been suggested that this may simply be an artifact of interpreting imprecisely measured cosmological data in the oversimplified framework of an universe assumed to be described by the exactly isotropic and homogeneous Friedmann-Robertson-Walker (FRW) metric, in which $H_0 \sim 10^{-42} \text{GeV} \sim (10^{28} \text{cm})^{-1}$ is the *only* scale [20]. Note that the non-zero value of $\Omega_\Lambda \equiv \Lambda/3H_0^2$ is inferred from the “cosmic sum rule” $\Omega_m + \Omega_K + \Omega_\Lambda = 1$, which is just a restatement of the Friedmann equation. If however this equation does not describe the real universe exactly, and in order to do so *other* non-zero terms ought to have been added to the sum rule, then we may mistakenly infer a value for Ω_Λ of $\mathcal{O}(1)$ if these other terms are in fact important. For example, in an inhomogeneous universe averaged quantities satisfy modified Friedmann equations which contain extra terms since the operations of spatial averaging and time evolution do not commute [21]. These “backreaction” terms depend upon the variance of the local expansion rate and hence increase as inhomogeneities develop. However although backreaction behaves just like a cosmological constant, whether its expected magnitude can indeed account for the apparent cosmological acceleration is debated and remains an open question at present [22–31].

Another possibility is that inhomogeneities affect light propagation on large scales and cause the luminosity distance-redshift relation to resemble that expected for an accelerating universe. This has been investigated for a “Swiss-cheese” universe in which voids modelled by patches of Lemaitre-Tolman-Bondi (LTB) space-time are distributed throughout a homogenous background. However, the results depend on the specific model: some authors find the change in light propagation to be negligible because of cancellation effects [32–35], whereas others claim it can partly mimic dark energy [36–38]. It may be that observers preferentially choose sky regions with underdense foregrounds when studying distant objects such as SNe Ia, so the expansion rate along the line of sight is then greater than average; such a selection effect may also allow an inhomogeneous universe to fit the observations without dark energy [39].

In this paper we are mainly interested in a “local void” (sometimes referred to as “Hubble bubble”) as an explanation for dark energy; to prevent an excessive CMB dipole moment due to our peculiar velocity we must be located near the centre of the void. An underdense void expands faster than its surroundings, thus younger supernovae inside the void would be observed to be reced-

ing more rapidly than older supernovae outside the void. Under the assumption of homogeneity this would lead to the mistaken conclusion that the expansion rate of the universe is accelerating, although both the void and the global universe are actually decelerating. The local void scenario has been investigated by several authors using a variety of methods [40–65]. By modelling the void as a open FRW region joined by a singular mass shell to a FRW background, it was found that a void with radius 200 Mpc can fit the supernova Hubble diagram without dark energy [46]. It was also shown that a LTB region which reduces to a EdS cosmology with $h = 0.51$ at a radius of 1.4 Gpc can match both the supernova data and the location of the first acoustic peak in the CMB [51]. Ref.[59] attempted to find the smallest possible void consistent with the current supernova results — their LTB-based ‘minimal void’ model has a radius of 350 Mpc. Unfortunately, since this model is equivalent to an EdS universe with $h = 0.44$ *outside* the void where the SDSS luminous red galaxies lie, as it stands it is unable to fit the measurements of the baryonic acoustic oscillation (BAO) peak at $z \sim 0.35$ [66]. LTB models of much larger voids were considered in Ref.[62] (with radii of 2.3 Gpc and 2.5 Gpc and Hubble contrasts of 0.18 and 0.30 respectively) and it was demonstrated they can fit the BAO data, as well as the SNeIa data and the location of the first CMB peak. Ref.[64] found the best fit to the SNe Ia data for a void of radius 1.3 ± 0.2 Gpc and Ref.[65] confirmed that such a void provides an excellent fit to the “Union” dataset of SNe Ia.

In this paper we demonstrate that, contrary to the results obtained in Refs. [67–70], a Gpc-sized void can simultaneously fit the SNe Ia data as well as the full CMB power spectrum, while also satisfying constraints from local Hubble measurements, primordial nucleosynthesis and the BAO data, if the primordial power spectrum is *not* assumed to be nearly scale-invariant. The layout of the paper is as follows. In Sec. II we summarize the general relativistic framework for LTB models and describe the characterization of the void. In Sec. III we discuss the form of the primordial power, and present a physical model with a primordial power spectrum that is not scale-free. In order to compare observables in the void model to existing cosmological data, some formalism needs to be developed. This is done in Sec. IV, and the statistical approach is discussed in Sec. V. Finally Sec. VI presents the main results of the paper.

II. LTB VOID MODELS

A. The metric and solution

We model the void as an isotropic, radially inhomogeneous universe described by the LTB metric:

$$ds^2 = -c^2 dt^2 + \frac{A^2(r, t)}{1 + K(r)} dr^2 + A^2(r, t) d\Omega^2, \quad (1)$$

where a prime denotes the partial derivative with respect to coordinate distance r , and the curvature $K(r)$ is a free function, bounded by $K < 1$. This reduces to the usual FRW metric in the limit where $A(r, t) \rightarrow a(t)r$ and $K(r) \rightarrow \kappa r^2$.

We define two Hubble rates:

$$H_{\perp} \equiv \frac{\dot{A}(r, t)}{A(r, t)}, \quad H_{\parallel} \equiv \frac{\dot{A}'(r, t)}{A'(r, t)}, \quad (2)$$

where an overdot denotes the partial derivative with respect to t . The analogue of the Friedmann equation is

$$H_{\perp}^2 = \frac{F(r)}{A^3(r, t)} + \frac{c^2 K(r)}{A^2(r, t)}, \quad (3)$$

where $F(r) > 0$ is another free function which determines the local energy density through

$$8\pi G\rho(r, t) = \frac{F'(r)}{A^2(r, t)A'(r, t)}. \quad (4)$$

We define dimensionless density parameters $\Omega_M(r)$ and $\Omega_K(r)$ such that

$$F(r) = H_0^2(r)\Omega_M(r)A_0^3(r), \quad (5)$$

and

$$c^2 K(r) = H_0^2(r)\Omega_K(r)A_0^2(r), \quad (6)$$

where $H_0(r)$ and $A_0(r)$ are the values of $H_{\perp}(r, t)$ and $A(r, t)$ respectively at the present time $t = t_0$. The Friedmann equation then becomes [71]:

$$H_{\perp}^2 = H_0^2 \left[\Omega_M \left(\frac{A_0}{A} \right)^3 + \Omega_K \left(\frac{A_0}{A} \right)^2 \right], \quad (7)$$

so $\Omega_M(r) + \Omega_K(r) = 1$. This equation can be integrated from the time of the Big Bang, $t_B = t_B(r)$, to yield the age of the universe at any given (r, t) :

$$t - t_B(r) = \frac{1}{H_0(r)} \int_0^{A/A_0} \frac{dx}{\sqrt{\Omega_M(r)x^{-1} + \Omega_K(r)}}. \quad (8)$$

We thus have two functional degrees of freedom, in $\Omega_M(r)$ and $t_B(r)$, which can be chosen as desired. (The third function, $A_0(r)$, corresponds to a gauge mode and we choose to set $A_0(r) = r$.) A spatially varying t_B corresponds to a decaying mode [72], so for simplicity we set $t_B = 0$ everywhere, so that at the current time t_0 :

$$H_0(r) = \begin{cases} \frac{-\sqrt{-\Omega_K} + \Omega_M \sin^{-1} \sqrt{-\frac{\Omega_K}{\Omega_M}}}{t_0 (-\Omega_K)^{3/2}}, & \Omega_K < 0; \\ \frac{2}{3t_0}, & \Omega_K = 0; \\ \frac{\sqrt{\Omega_K} - \Omega_M \sinh^{-1} \sqrt{\frac{\Omega_K}{\Omega_M}}}{t_0 \Omega_K^{3/2}}, & \Omega_K > 0. \end{cases} \quad (9)$$

The void model can then be specified by the choice of one free function, which we take to be $\Omega_M(r)$, and a constant $H \equiv H_0(0)$ which determines the *local* Hubble rate at the centre (and is equivalent to choosing t_0). Note that both at the centre of the void and far outside the void, the definition of $\Omega_M(r)$ reduces to the standard FRW density parameter Ω_m .

The solution to Eq.(7) for general r and t can be given in parametric form for the different values of $\Omega_K(r)$ (or $K(r)$) as follows [42]:

- for $\Omega_K(r) > 0$:

$$A = \frac{\Omega_M(r)A_0(r)}{2\Omega_K(r)} (\cosh \eta - 1), \quad (10a)$$

$$H_0 t = \frac{\Omega_M(r)}{2\Omega_K^{3/2}(r)} (\sinh \eta - \eta). \quad (10b)$$

- for $\Omega_K(r) = 0$:

$$A = \frac{1}{2} (18\Omega_M(r))^{1/3} (H_0 t)^{2/3} A_0(r). \quad (11)$$

- for $\Omega_K(r) < 0$:

$$A = \frac{\Omega_M(r)A_0(r)}{2|\Omega_K(r)|} (1 - \cos u), \quad (12a)$$

$$H_0 t = \frac{\Omega_M(r)}{2|\Omega_K(r)|^{3/2}} (u - \sin u). \quad (12b)$$

Light travels to an observer at the centre of the void along null radial incoming geodesics described by [42]:

$$\frac{dt}{dz} = -\frac{1}{(1+z)H_{\parallel}(z)}, \quad (13a)$$

$$\frac{dr}{dz} = \frac{c\sqrt{1+K(r)}}{(1+z)A'(z)H_{\parallel}(z)}, \quad (13b)$$

where $H_{\parallel}(z) = H_{\parallel}(r(z), t(z))$ etc. The angular diameter distance at redshift z is then given by

$$d_A(z) = A(r(z), t(z)), \quad (14)$$

and the luminosity distance by

$$d_L(z) = (1+z)^2 A(r(z), t(z)). \quad (15)$$

All observable quantities along the light cone can be calculated from these equations.

B. Void profile

We can now choose the void profile by specifying $\Omega_M(r)$ and the local value of the Hubble rate by specifying H . Although the void profile may have any shape, we restrict ourselves to the simple Gaussian form:

$$\Omega_M(r) = \Omega_{\text{out}} - (\Omega_{\text{out}} - \Omega_{\text{in}}) \exp \left[-\left(\frac{r}{r_0} \right)^2 \right], \quad (16)$$

where Ω_{in} and Ω_{out} correspond to the matter density parameter at the centre of the void and at infinity, respectively, and r_0 characterizes the width of the void. We wish to look only at voids that are asymptotically EdS, so we set $\Omega_{\text{out}} = 1$. Thus distances in the void model are completely specified by the three parameters Ω_{in} , r_0 and H .

We wish to stress that in restricting ourselves to voids which have a Gaussian profile, we may be missing the model that fits the data best. In principle we could sample a wider class of profiles and choose the form that gives the best fit. However in this paper we are concerned mainly with providing a counter-example of a void which can simultaneously fit both the SNe Ia magnitudes and the CMB spectrum, so we do not perform this search.

III. PRIMORDIAL POWER SPECTRA

The observed power spectrum of CMB anisotropies in any cosmological model is a convolution of three unknowns. The first two are the local physics at the time of recombination, which is dependent on the composition of the universe at that time, and the angular diameter distance to the last scattering surface (LSS), which depends on the geometry of the universe. Both of these are completely specified by the choice of the void model as described in Section II B, along with the further specification of the baryon fraction, Ω_b and the baryon-to-photon ratio $\eta \equiv n_b/n_\gamma$.

The third unknown is the shape of the primordial power spectrum of density perturbations. In toy models of inflation this is close to scale-invariant and featureless. Under the assumption that the primordial spectrum is described by a simple power law, the standard Λ CDM concordance cosmological model fits the observed angular power spectrum reasonably well [73]. However, there is no independent evidence for this form of the primordial power and as the observed anisotropies arise as a convolution of the *assumed* primordial spectrum with the transfer function of the *assumed* cosmological model, it is clear that we cannot determine one without making assumptions about the other. (In fact, there are indications that the primordial spectrum is *not* scale-free, even when a Λ CDM cosmology is assumed [74–83].)

In Refs. [67–70] it is argued that, *assuming near-scale invariance of the primordial power*, void models cannot simultaneously provide an explanation for supernovae magnitudes and fit the observed CMB spectrum, unless the void is extremely deep [67] or embedded in a universe with large non-zero overall curvature [70]. However, in considering void models as an alternative to dark energy, we are in any case departing from the concordance cosmology, so there is no need to retain the assumption that the primordial power spectrum is scale-free. If this assumption is relaxed then even an EdS cosmology *without* dark energy can fit the CMB data [17, 19]. In this paper we consider a particular alternative form of the primor-

dial $\mathcal{P}(k)$ that is not scale-free but is in fact physically well-motivated, as described below.

A. Bump model

Whereas the simplest toy models of inflation contain only a single scalar field which rolls slowly down its potential, *physical* models generically contain other fields, whose evolution is typically not slow-roll. These fields may couple to the inflaton and affect its evolution, thus breaking the scale-free nature of the primordial power, with important consequences.

An example of such a physical model is “multiple inflation” [84] in the framework of $N = 1$ supergravity, the locally realised version of supersymmetry (SUSY). This model includes “flat-direction” fields ψ which have gauge and Yukawa couplings to ordinary matter but are only gravitationally coupled to the inflaton. Such flat-directions have been classified and tabulated in the Minimal Supersymmetric Standard Model (MSSM) [85]. As the universe cools during inflation, the ψ fields undergo symmetry-breaking phase transitions, causing a sudden change in the effective mass of the inflaton (which is assumed to be a field in a “hidden sector”). For a single flat-direction field, this produces a ‘step’ in the spectrum of the curvature perturbation [86]. If more than one flat-direction field is present, they can couple to the inflaton with opposite signs, and instead produce a ‘bump’ feature in the power spectrum [17]. (A toy model that produces a similar “step” feature in the power spectrum has also been proposed [87] and has been studied with respect to fitting the WMAP 1-year [88, 89] and 3-year [90] data, albeit in a different context to that considered here. Other signatures of multiple inflation, in particular the generation of associated non-Gaussianities, have also been studied [91].)

The potential for the inflaton ϕ and the flat-direction fields ψ_i is then given by

$$V(\phi, \psi_1, \psi_2) = V_0 - \frac{1}{2}m^2 H_1^2 \phi^2 + \frac{1}{2}\lambda_1 H_1^2 \phi^2 \psi_1^2 - \frac{1}{2}\mu_1^2 H_1^2 \psi_1^2 + \gamma_1 \psi_1^{n_1} + \frac{1}{2}\lambda_2 H_1^2 \phi^2 \psi_2^2 - \frac{1}{2}\mu_2^2 H_1^2 \psi_2^2 + \gamma_2 \psi_2^{n_2}, \quad (17)$$

where mH_1 and $\mu_i H_1$ are the masses of the ϕ and ψ_i fields respectively, $\lambda_i H_1^2$ is the coupling of the ψ_i field to the inflaton, γ_i is the coefficient of the non-renormalizable operator of order n_i which lifts the potential of the ψ_i field and H_1 is the Hubble scale during inflation (units of Planck mass $M_P = 1$ are used throughout). The two flat-direction fields remain trapped at the origin by thermal effects until the phase transitions take place at times t_i . Natural values for the parameters of this model are $|\lambda_i| \sim 1$, $\mu_i^2 \sim 3$, and $\gamma_i \sim 1$. According to the list of flat-direction fields in Ref. [85], the ones with $n_i = 12, 16$ will be the most relevant. It is usually assumed that

some symmetry protects the inflaton mass m from SUSY-breaking corrections (the “ η problem”), thus allowing sufficient e-folds of inflation to occur. Note that the times of the phase transitions t_1 and t_2 — or, equivalently, the scales k_1 and k_2 at which the effects of the flat-direction fields begin to be felt — are however arbitrary.

In Ref. [17] a full likelihood analysis was performed to demonstrate that a primordial power spectrum with such a ‘bump’ would allow even an EdS universe with $\Lambda = 0$ to fit the WMAP 3-year data, although this requires a rather low value of $h_0 \simeq 0.44$. As void models generically imply a lower global value of h_0 than the local value at the centre where we are located, such a primordial power spectrum could help a void model to fit the CMB.

The primordial power spectrum produced by this ‘bump’ model can be calculated exactly by numerically solving the equation of motion of the ϕ field according to the potential in Eq.(17). However, we do not choose to do so for two reasons. Firstly, this evaluation is computationally expensive and slows an MCMC analysis considerably. Secondly, our results regarding void models are dependent only on the existence of such a feature, rather than the details of the particular theory that explains it. Multiple inflation provides an example of such a theory, but similar features with steps and oscillations may also be produced, *e.g.*, in DBI inflation [92]. Strictly speaking it is not even necessary to assume that these features arise from an inflationary model at all.

With this in mind, we introduce a parameterization of the primordial scalar power $\mathcal{P}(k)$ to capture the essential features of the ‘bump’ model instead of attempting to reproduce it exactly:

$$\mathcal{P}(k) = \mathcal{P}_0 \left(1 - a \tanh(bx) + ce^{-(bx)^2} \right), \quad (18)$$

where $x \equiv \log_{10}(k/k_0)$. In Fig. 1 we plot $\mathcal{P}(k)$ obtained from a full calculation in the “bump” model, with parameter values $n_1 = 16$, $n_2 = 12$, $\mu_1^2 = \mu_2^2 = 3$, $\gamma_1 = \gamma_2 = 1$, $\lambda_1 = -0.2$, $\lambda_2 = 1$ and $m^2 = 0.05$ (all set at their “natural” values, save for λ_1). H_1 , k_1 and k_2 are free parameters and are chosen so as to broadly reproduce the best-fit primordial spectrum from Ref. [17]. In the same figure we also plot the form of our simple parameterization. We do not consider any tensor modes, as in “small field” models such as multiple inflation these are always negligibly small.

This form of $\mathcal{P}(k)$ is thus determined by 5 free parameters: \mathcal{P}_0 , a , b , c and k_0 . This may appear to be a step backwards from the standard power-law form, which depends on only 3 (A_S , n_s and n_{run} — the amplitude, slope and “running” of the spectrum). However it is important to bear in mind that we are merely using an empirical parameterization for a $\mathcal{P}(k)$ that is ultimately the result of some underlying theory, in which all of these parameters are in fact determined by fundamental physics.

On the other hand, it can be argued that the standard parameterization of a power-law hides other parameters which are artificially set to zero through the overriding

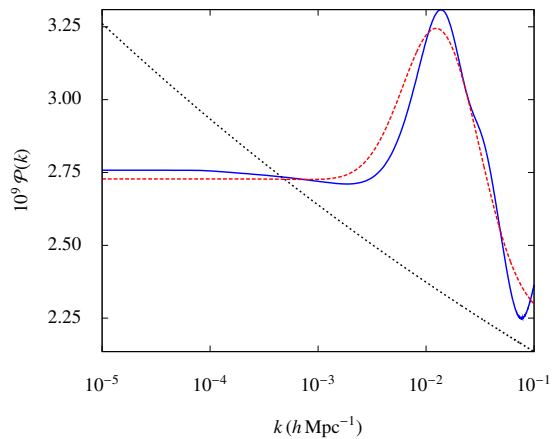


FIG. 1. The solid (blue) curve shows the primordial power spectrum obtained from a full calculation of the multiple inflation model, with parameters as described in the text. The dashed (red) curve shows the simple parameterization (18), with parameter values $\mathcal{P}_0 = 2.48 \times 10^{-9}$, $a = 0.1$, $b = 2.0$, $c = 3.0$ and $k_0 = 0.015$. For comparison, the dotted (black) curve shows a standard power-law spectrum with slope $n_s = 0.954$, amplitude $A_S = 2.3 \times 10^{-9}$, which are the best-fit values for the Λ CDM model with no “running” to the CMB+SN_{CFA} datasets (Sec. VI).

assumption that only a single scalar field is involved. In the absence of an accepted physical mechanism for inflation, we feel that all plausible alternatives ought to be considered, rather than judging purely on the basis of naive parameter-counting. It is with this rationale that we use this form of the primordial power in constructing our counter-example.

IV. FITTING THE MODEL TO OBSERVATIONS

In this section we will discuss how to fit the void model to the best available cosmological data: the WMAP 7-year release [73], SNe Ia data from the Constitution [93] and the Union2 compilation [94], the local Hubble rate measurement by the Hubble Key Project [95], constraints from big bang nucleosynthesis [96], and BAO measurements from SDSS DR7 [97].

As cosmology in an LTB metric differs from the standard FRW approach, we need to develop some formalism to allow us to confront these datasets in a consistent manner. This is outlined in the following.

A. SNe Ia magnitudes

The distance modulus of a supernova is defined as the residual between its apparent and absolute magnitudes m and M , and is related to its luminosity distance as

$$\mu = m - M = 5 \log_{10} \left[\frac{d_L}{\text{Mpc}} \right] + 25, \quad (19)$$

so that, knowing μ for each object in a dataset, we can use Eq.(15) to compare a void model to the data.

We use two datasets: the Constitution compilation of 397 SNe in the redshift range $z = 0.015 - 1.55$ [93] and the Union2 compilation of 557 SNe in the range $z = 0.015 - 1.4$ [94]. The Constitution sample uses the SALT lightcurve fitter while Union2 uses the newer SALT2 fitter. Neither fitter, however, directly provides the value of μ for each object — for instance, the SALT fitter provides as output values of m_B^{\max} (the rest-frame peak magnitude in the B-band), a time stretch factor, s , and a colour parameter, c , for each supernova, from which the distance modulus is calculated as:

$$\mu_i = m_{B,i}^{\max} - M + \alpha \cdot (s_i - 1) - \beta \cdot c_i, \quad (20)$$

where M , α and β are empirical coefficients whose values are determined by marginalizing over the fit to a particular fiducial cosmology. The SALT2 fitter follows the same principle, though with a ‘stretch factor’, x_1 , that is analogous to but not the same as s .

Both the Constitution and Union2 compilations provide tabulated values of distance modulus μ and its estimated error σ_μ for a choice of coefficients M , α and β calculated for the best-fit flat Λ CDM model. In addition, σ_μ includes an important contribution from a systematic uncertainty whose value is *chosen* such that the reduced χ^2 value for the flat Λ CDM model is of order unity. Hence when comparing any alternative model to Λ CDM on the basis of their respective fits to the SNe Ia data, we ought to in principle perform the entire fitting analysis from scratch, choosing the values of M , α and β that produce the best fit for the particular model under consideration, and adjusting the systematic error inserted by hand in an equivalent manner. However, to do so we would require not only the actual lightcurve fitter outputs for each supernova (which the publicly downloadable data for the Constitution set does contain, but Union2 does not), but also the full covariance matrix of the lightcurve fits, which neither compilation provides.¹ Therefore, we are forced to adopt the common (if incorrect) procedure of fitting the void model by marginalizing over the unknown absolute magnitude M alone, while bearing in mind the caveat that this may bias our results and our best-fit void parameters in an unknown manner.

B. CMB power spectrum

It has been shown in several previous studies that void models are only very loosely constrained by the position of the first peak of the CMB [51, 62]. However, the WMAP satellite has in fact measured the angular power spectrum C_l s over a wide range of multipoles, l , and it is

preferable to use as much of this data as possible. This entails the calculation of the full predicted C_l spectrum for the void model. This has been done using various methods [67–70], but always with the assumption of a nearly scale-invariant primordial spectrum.

In order to be able to calculate the predicted angular power spectrum for an LTB model using one of the publically available Boltzmann codes (we use a version of CAMB [99], modified to accept the primordial power spectra we consider), we use a version of the “effective EdS approach” [68, 69]. In brief, this consists of constructing an effective EdS model which has the same physics at recombination as the given void model, and the same angular diameter distance to the LSS. Then, given the same primordial power spectrum, the C_l s of the effective model and the void model will be the same, at intermediate and small angular scales. Thus the effective model can be used as a calculational tool to obtain the power spectrum for the void model under consideration. Note however that the effective EdS model will in general have a central temperature, T_0^{EdS} , and a central Hubble rate, H_0^{EdS} , that are *different* from the actual T_0 and H_0 that we observe today. This is because the physics has been matched at early times; at late times the models must then necessarily differ.

To generate the effective model, we adopt the following procedure. First we specify the void profile and local Hubble rate by choosing the parameters Ω_{in} , r_0 and H . Then, using Eqs. 13a) and (13b) we numerically integrate out from the centre of the void along the past light cone to obtain the coordinates (r_m, t_m) at an intermediate redshift z_m . As in Refs. [68, 69] we choose this redshift to be $z_m = 100$, where the spatial curvature of the void is negligible but the radiation density is still small and can justifiably be ignored in the calculations.

At these coordinates we now calculate the Hubble rate, $H_m = H_{\perp/\parallel}(r_m, t_m)$ and the angular diameter distance $A_m = A(r_m, t_m)$. Let us denote by $r^{\text{EdS}}(t)$ the comoving radial coordinate of a radial light ray in the EdS universe and by z^{EdS} the redshifts seen by an observer at $r^{\text{EdS}} = 0$. To ensure the matching of the distances to the LSS, we impose the condition $A_m = a(r_m^{\text{EdS}})r_m^{\text{EdS}}$ for EdS scale factor a . This provides us with the relation

$$A_m = \frac{2c}{(1 + z_m^{\text{EdS}}) H_0^{\text{EdS}}} \left(1 - \frac{1}{\sqrt{1 + z_m^{\text{EdS}}}} \right), \quad (21)$$

where z_m^{EdS} is the redshift in the EdS universe at coordinates (r_m^{EdS}, t_m) . (Note that our procedure implies $z_m^{\text{EdS}} \neq z_m$ and thus differs slightly from the equivalent method outlined in Refs.[68, 69] where instead $z_0^{\text{EdS}} \neq 0$.) To ensure the same physics at early times in the two models we also match the Hubble rates, $H_m = H^{\text{EdS}}(z_m^{\text{EdS}})$, and this combined with Eq.(21) provides us with an expression for z_m^{EdS}

$$z_m^{\text{EdS}} = \frac{A_m^2 H_m^2 + 4c A_m H_m}{4c^2}. \quad (22)$$

¹ This is provided in the SNLS 3-year data release [98]; however it contains only 231 objects, so we do not consider it here.

Given the value of z_m^{EdS} , we can then calculate the effective EdS mean temperature and Hubble rate via

$$T_0^{\text{EdS}} = T_0 \left(\frac{1 + z_m}{1 + z_m^{\text{EdS}}} \right), \quad (23a)$$

$$H_0^{\text{EdS}} = \frac{H_m}{(1 + z_m^{\text{EdS}})^{3/2}}, \quad (23b)$$

where $T_0 = 2.726 \pm 0.001$ K is the CMB temperature observed today [100].

The parameters $T_0^{\text{EdS}}, H_0^{\text{EdS}}, \Omega_m = 1, \Omega_\Lambda = \Omega_K = 0$ and the baryon fraction Ω_b can then be fed into CAMB, together with the choice of primordial power spectrum, to find the spectrum of C_l s for the effective EdS model. This will be identical to the spectrum actually observed at the centre of the void, at large enough values of l .

At small values of l however, the void model will create an integrated Sachs-Wolfe (ISW) signal which is not captured by the effective EdS model. However, no rigorous calculation has yet been made of this expected ISW signal. In addition, the void may also in principle have a different reionization history than that of the effective EdS model. These two effects mean that at small l the C_l values calculated using the EdS model will differ, in both the TT and TE power spectra, from the actual spectrum due to the void.

In order to account for this, we choose to apply a cutoff at $l = 32$ in both the WMAP-7 TT and TE power spectra. The value $l = 32$ is chosen also to coincide with the switch-over point for the TT power spectrum at which the WMAP likelihood routine switches between the low- l , gibbs-sampling likelihood estimation technique and the master code for high- l (for the TE spectrum the switch-over point between pixel-based analysis and the master code is close by at $l = 24$). This also allows a more direct interpretation of the likelihood \mathcal{L} in terms of a χ^2 value. We have checked that increasing the cutoff point does not materially affect our results.

Given that in Ref. [17] it is found that an EdS model can fit the WMAP data with a primordial power spectrum similar to the ‘bump’ model we use here, we expect to find a good fit to the CMB with $h_0^{\text{EdS}} \equiv H_0^{\text{EdS}}/(100 \text{ kms}^{-1} \text{ Mpc}^{-1}) \simeq 0.44$ and $T_0^{\text{EdS}} \simeq T_0$. This should be contrasted with the values of $h_0^{\text{EdS}} \simeq 0.51$ and $T_0^{\text{EdS}} \simeq 3.4$ K required with a power-law primordial spectrum [68, 69].

C. Local Hubble rates

It has been claimed in previous studies [68–70] that the *local* Hubble rate of void models that fit the CMB and SNe Ia data simultaneously must be very low (as low as $h_0 \simeq 0.45$ in Refs. [68, 69]) and that this argues against void models, since the measured local values (at $z < 0.1$) are significantly higher (see Ref. [101] for a review). This can provide an important discriminant against void models. Therefore in performing the MCMC analysis, we

also fit the local Hubble rate for the void model $h_0^{\text{LTB}} \equiv H/100$ to the Hubble Key Project (HKP) value $h_0 = 0.72 \pm 0.08$ [95]. We note that there is some variation in the value of h_0 obtained by different groups, ranging from $h_0 = 0.623 \pm 0.06$ [102] to $h_0 = 0.742 \pm 0.036$ [103], and the HKP value lies in between these two.

The SNe Ia compilations, WMAP-7 observations and the HKP value for h_0 form the primary datasets that we use to constrain the void model. We also discuss the fit to some other cosmological data below.

D. Big bang nucleosynthesis

Our theoretical understanding of the physics of the epoch of big bang nucleosynthesis allows us to use observations of the abundances of various elements to constrain the baryon-to-photon ratio, $\eta = n_b/n_\gamma$, at that time. Although η is constant with time in FRW spacetime, this is not the case in LTB spacetime. However, assuming that η is spatially constant in the LTB model (which need not necessarily be true, see Refs. [104, 105]), we can use the effective EdS model to calculate η for the void model. Since both models share the same early universe physics by construction, we have [69]

$$\eta_{10} \equiv 10^{10} \eta = 273.9 \left(\frac{T_0}{T_0^{\text{EdS}}} \right)^3 \omega_b, \quad (24)$$

where $\omega_b \equiv \Omega_b (h_0^{\text{EdS}})^2$. The inferred primordial abundance of deuterium, together with that of helium, provides the constraint $5.1 \leq \eta_{10} \leq 6.5$ at 95% C.L. [96].

E. BAO scale

The BAO data provided by the SDSS collaboration [97] are essentially measurements of a feature in the correlation function of the observed galaxy distribution which is related to the physical sound horizon at the CMB scale, evolved down to the redshift at which the measurement is made. The full theory for how these perturbations should evolve in LTB spacetimes is unknown and a difficult problem, as the background curvature enters the Bardeen equation for the gravitational potential. As this may vary significantly over scales of ~ 150 Mpc, it can potentially add a significant and as yet unknown distortion to BAO scales [106].

Nevertheless, some efforts have been made to compare void models to BAO data under the assumption that the evolution of perturbations does *not* depend on scale (as is the case in FRW spacetime) [68–70]. Under this assumption the difference between LTB and FRW spacetimes is simply that as $H_\parallel \neq H_\perp$ for $r > 0$, physical length scales in an LTB spacetime evolve differently in radial and transverse directions at late times, whereas in FRW models the evolution is isotropic. It is not clear that this is necessarily a valid assumption to make. However, in

order to provide a comparison with the previous studies we follow the same prescription as in Ref. [69], while bearing in mind that a better calculation may lead to significant changes in the results.

The first step is to construct another effective EdS model, referred to as the “BAO model”, which shares the same early universe physics as the void model under consideration, but unlike in the previous case, need not match the angular diameter distance to the LSS. We choose in this case to match the central temperatures, $T_0^{\text{BAO}} = T_0$, which then provides us with the relation:

$$H_0^{\text{BAO}} = \frac{H_m}{(1+z_m)^{3/2}}, \quad (25)$$

as unlike in the previous Section, we will now have $z_m^{\text{BAO}} = z_m$ (where, as before, we choose $z_m = 100$). We also match the values of Ω_b and $\Omega_m = 1$ at this redshift to ensure the same early universe physics.

As the BAO model and the LTB void model have, by definition, the same physics at coordinates $(r(z_m), t(z_m)) \equiv (r_m, t_m)$, and since at this redshift the LTB spacetime is sufficiently close to FRW, we may conclude that the physical sound horizon in the void model at time t_m is essentially isotropic and homogeneous, and equal to the sound horizon $s_p(z_m)$ in the BAO model, which may be calculated according to [107]:

$$s_p(z) = \frac{44.5 \ln [9.83 / (\Omega_m h_0^2)]}{(1+z) \sqrt{1 + 10 (\Omega_b h_0^2)^{3/4}}} \text{Mpc}. \quad (26)$$

In order to evaluate the BAO scales observed at redshift z by an observer at the centre of the void, we need to evolve this physical sound horizon scale down to coordinates $(r(z), t(z))$ in the LTB background. Thus the radial and transverse physical BAO scales at redshift z will be, respectively,

$$l_{\parallel}^{\text{BAO}}(z) = s_p(z_m) \frac{A'(r(z), t(z))}{A'(r(z), t_m)}, \quad (27)$$

$$l_{\perp}^{\text{BAO}}(z) = s_p(z_m) \frac{A(r(z), t(z))}{A(r(z), t_m)}, \quad (28)$$

and these can in turn be rewritten in terms of the corresponding redshift and angular intervals:

$$\Delta z(z) = (1+z) l_{\parallel}^{\text{BAO}}(z) H_{\parallel}(r(z), t(z)), \quad (29)$$

$$\Delta \theta(z) = \frac{l_{\perp}^{\text{BAO}}}{A(r(z), t(z))}. \quad (30)$$

It is these values of $\Delta z(z)$ and $\Delta \theta(z)$ that are directly measurable. As mentioned in Ref. [69], the redshift scale $\Delta z(z)$ is expected to be a stronger discriminator of void models than $\Delta \theta(z)$. However, while estimates of the radial BAO scale have been made [108, 109], the statistical significance of these claims has been questioned [110, 111]. Given this ambiguity, we choose not to use this data; instead we use constraints on the ratio,

$$\Theta(z) \equiv \frac{s_p(z_{\text{rec}})}{D_V(z)}, \quad (31)$$

at redshifts $z = 0.2$ and $z = 0.35$ from Ref. [97], where z_{rec} is the redshift at recombination and $D_V(z)$ is an isotropized distance measure. This is given in a FRW model by [10]

$$D_V^{\text{FRW}}(z) \equiv \left[\frac{z d_A^2(z)}{H(z)} \right]^{1/3}, \quad (32)$$

where $d_A(z)$ and $H(z)$ represent, respectively, the angular diameter distance and the Hubble rate in the FRW model.

As the BAO measurements are quoted in terms of the ratio $\Theta(z)$, it is necessary to convert them into a form that can be related to $\Delta z(z)$ and $\Delta \theta(z)$. It can be shown [70] that

$$Q(z) \equiv (\Delta \theta^2 \Delta z)^{1/3} = z^{1/3} \Theta(z), \quad (33)$$

and this is the measure we use to compare the void model to the data.

V. METHOD

We perform a likelihood analysis using COSMOMC [112] to generate Markov-Chain-Monte-Carlo (MCMC) chains to estimate confidence limits on the parameters in fitting the model to the data. For each void model, specified by Ω_{in} , r_0 and H , we first calculate the effective parameters H_0^{EdS} and T_0^{EdS} as described in Sec. IV B. We fix the optical depth to the LSS to the WMAP-7 value, although this choice is immaterial as our cutoff at $l = 32$ means that the data do not constrain reionization in any case. Therefore the full set of parameters for the void model is: local matter density Ω_{in} , void radius r_0 , local Hubble value H , baryon fraction Ω_b , and the power spectrum parameters \mathcal{P}_0 , a , b , c and k_0 . (The cold dark matter density Ω_c is set equal to $1 - \Omega_b$ since we are not considering large-scale structure formation here so do not need to invoke a small component of hot dark matter to match the SDSS power spectrum of galaxy clustering as in Ref.[17].) These are fed as inputs to CAMB [99] to generate the CMB spectrum for the model.

Once the output C_l values have been obtained from CAMB, we can fit the model to the WMAP-7 data [73], the SNeIa data (the Constitution [93] and Union2 [94] datasets are fitted separately), the HKP value for the local Hubble rate [95], the BAO data [97] and the BBN constraint [96].

In order to compare the goodness of fit, we perform exactly the same fitting procedure for a vanilla Λ CDM model whose parameters are: baryon density $\Omega_b h_0^2$, cold dark matter density $\Omega_c h_0^2$, local Hubble rate $100 h_0$,² and

² The COSMOMC code actually uses the ratio of the sound horizon to the angular diameter distance as the input parameter, but this is equivalent to using h_0 .

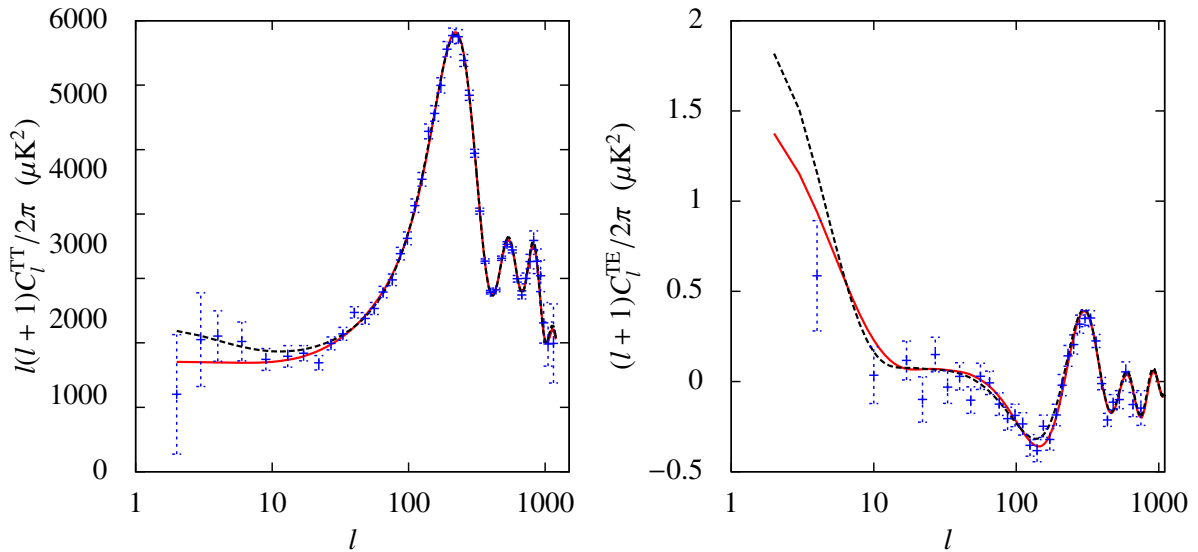


FIG. 2. The TT and TE power spectra of the models that best fit the CMB and Constitution SNeIa data. The solid (red) curve is for the void model, calculated using the effective EdS approach described in Sec. IV B, and the dashed (black) curve is for Λ CDM. Binned WMAP-7 data is also shown.

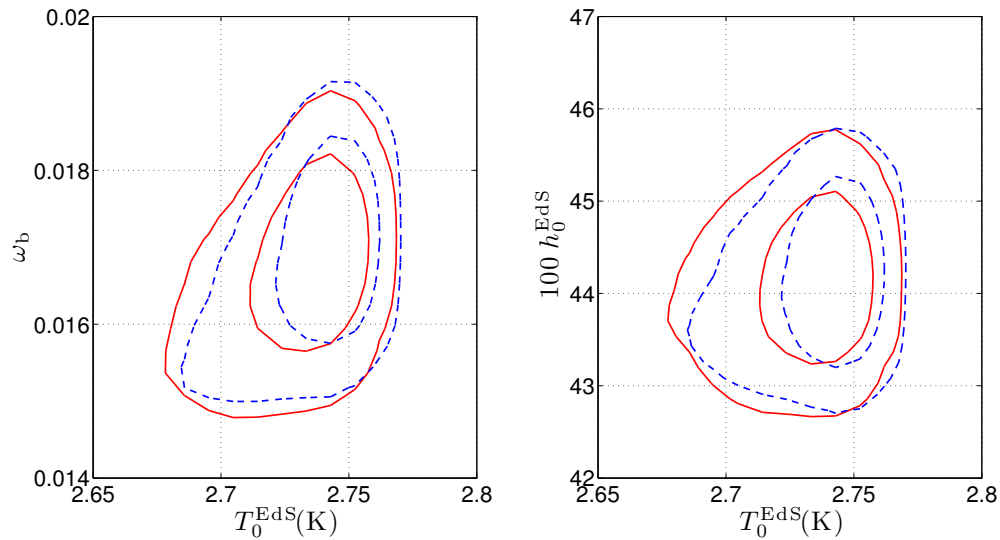


FIG. 3. Constraints on the effective EdS parameters for the void model with a bump, from CMB and SNe Ia data. The solid (red) contours show the 1 and 2σ likelihood confidence intervals for the Constitution SNe Ia data set and the dashed (blue) contours are for Union2.

the power spectrum amplitude, A_S , and slope, n_s . We characterize the best-fit likelihood of the void model by the value $\Delta\chi^2 = -2\ln(\mathcal{L}_{\text{void}}/\mathcal{L}_{\Lambda\text{CDM}})$, which means that negative values of $\Delta\chi^2$ favour the void. In Fig. 2 the TT and TE power spectra are shown for two sample best-fit models. The quantitative results of the analysis are discussed in the next section.

VI. RESULTS

In this section we shall use SN_{CfA} to denote the Constitution data set and SN_{U2} to denote Union2; CMB denotes the WMAP-7 data and HKP the Hubble Key Project value for the Hubble rate.

In Figure 3 we plot the 2D likelihoods for the effective EdS model parameters T_0^{EdS} , H_0^{EdS} and ω_b obtained from the MCMC chains for both CMB+ SN_{CfA} and CMB+ SN_{U2} data. Clearly, $T_0^{\text{EdS}} \simeq T_0$ and $h_0^{\text{EdS}} \simeq 0.45$, which is exactly as we expect, given the results of

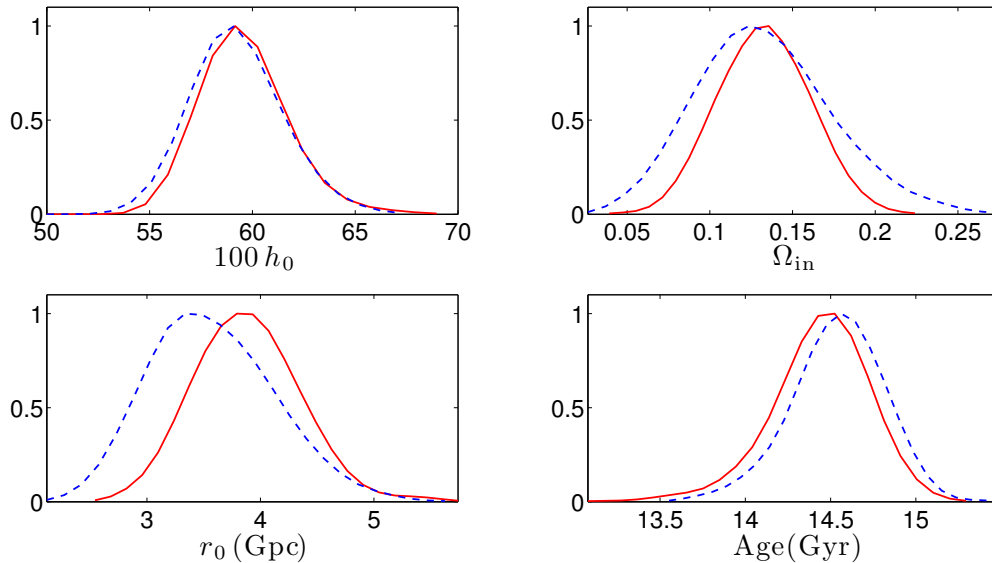


FIG. 4. Marginalized 1D likelihoods for the void model with a bump, for the fit to CMB and SNe Ia data. The solid (red) curves are for the Constitution SNe Ia data set and the dashed (blue) curves are for Union2.

Ref. [17]. Figure 4 shows the marginalized likelihoods of the void parameters and the resultant age of the universe, for the same datasets.

For both CMB+SN_{CfA} and CMB+SN_{U2} we obtain a local Hubble value $h_0 \sim 0.60 \pm 0.02$, which, although slightly low, is still consistent with the HKP value of $h_0 = 0.72 \pm 0.08$ to within 2σ . It is also much higher than the value of h_0 obtained in previous studies [68, 69]. This is because in order to fit the CMB with a power-law primordial spectrum a value of $T_0^{\text{EdS}} \simeq 3.4$ K is required and in order to generate this, the void must be surrounded by a large over-dense shell. The presence of this shell means the asymptotic value $H_0(r \gg r_0) \sim H_0^{\text{EdS}} \sim H_0(0)$ and hence in order to fit the CMB, $H_0(0)$ must be small. In contrast, our void profile does not have an over-dense shell, and as shown in Figure 3, $T_0^{\text{EdS}} \simeq T_0$. This allows us to generate the difference between $h_0 \simeq 0.60$ and $h_0^{\text{EdS}} \simeq 0.45$.

Our void model also does not suffer from the “old age” problem referred to in Ref.[69]: we find the age of the void universe to be 14.4 ± 0.3 Gyr for the CMB+SN_{CfA} chains and 14.5 ± 0.3 Gyr for CMB+SN_{U2}, which are significantly less than the values of ~ 18.8 Gyr quoted in [69]. This is unsurprising as the age t_0 is related to the value of h_0 by Eq. 9, and reasonable values for one ensure reasonable values for the other.

To enable a comparison of the quality of the fits, we show in Table I the $\Delta\chi^2$ values for the best-fit model with a void and a spectral “bump”, relative to the standard Λ CDM model, for different combinations of the primary constraining data sets. It is clear that the $\Delta\chi^2$ values in all cases are small given the number of degrees of freedom involved, which shows that the void model is

TABLE I. Best-fit likelihood values for Λ CDM and the relative $\Delta\chi^2$ values for the void model with a spectral ‘bump’ for different choices of the fundamental constraining data sets. Here SN_{CfA} refers to the Constitution sample and SN_{U2} to Union2. CMB refers to WMAP-7 data and HKP to the Hubble Key Project value for h_0 . Constitution data favour the void slightly and Union2 data favour Λ CDM slightly, but neither difference is significant given the number of degrees of freedom.

Datasets	# d.o.f.	$-2\ln(\mathcal{L}_{\Lambda\text{CDM}})$	$\Delta\chi^2$
CMB	1936	5785.0	+0.9
CMB + SN _{CfA}	2333	6250.4	-3.3
CMB + SN _{U2}	2493	6315.7	+1.4
CMB + SN _{CfA} + HKP	2334	6250.5	-0.6
CMB + SN _{U2} + HKP	2494	6315.9	+3.4

perfectly compatible with these datasets. A more quantitative comparison cannot be made because as noted in Sec. IV A the SNe Ia data are adjusted to fit a fiducial Λ CDM model and the error bars are tuned to give a χ^2 per degree of freedom of order unity for this model.

It should be noted that the addition of the HKP constraint increases the $\Delta\chi^2$ value by ~ 2 for Union2 and ~ 2.7 for Constitution, which reflects the fact that CMB and SNe Ia data favour a value of h_0 that is consistent with, but lower than, the HKP value. Even with this increase however, the $\Delta\chi^2$ values are still small (and in fact the void provides a marginally better fit to the CMB+SN_{CfA} data than does Λ CDM). It is possible that a thorough exploration of possible void profiles or use of unbiased SNe Ia data will make this fit better, but as this

does not detract from the main results presented here, we do not investigate it in this paper.

A more interesting constraint comes from Big Bang nucleosynthesis. From our MCMC chains for CMB+SN_{CfA} and CMB+SN_{U2} we find in both cases $\eta_{10} = 4.6 \pm 0.2$, which is $\sim 2\sigma$ below the best-fit value. This arises primarily because ω_b is on the low side, as seen in Figure 3. When the BBN constraint is added to the MCMC chains, we find an increase in $\Delta\chi^2$ of ~ 2.5 relative to the values for CMB+SN_{CfA}+HKP and an increase of ~ 3.1 for CMB+SN_{U2}+HKP. It should be noted however that the inferred primordial abundance of lithium indicates a significantly lower value of η than does deuterium [96], hence a better understanding of the chemical evolution of these fragile elements is required before the significance of the marginal discrepancy above can be assessed.

Finally, we find that adding the BAO data results in an increase in $\Delta\chi^2$ of 4.9 relative to the value for CMB+SN_{U2}+HKP+BBN and 5.5 relative to the value for CMB+SN_{CfA}+HKP+BBN, for an additional two degrees of freedom. The main reason for this increase is that the BAO data require a shallower void with $\Omega_{in} \sim 0.17$, whereas the CMB+SN data favour a slightly deeper void with $\Omega_{in} \sim 0.13$. Most of the increase in χ^2 arising from including the BAO data comes from the poorer fit to SNe Ia data that results. Given the uncertainty in interpreting χ^2_{SN} that we have already mentioned, as well as the assumptions that have gone into our analysis in Sec. IV E, we cannot draw any definite conclusions from these results. However it would appear that the BAO data are certainly not inconsistent with a void model.

VII. DISCUSSION

An interesting proposed test of void models is the Compton y -distortion of the CMB spectrum that is produced by the scattering of photons by reionized gas in regions of the void that see a highly anisotropic LSS [58]. In the single-scattering and linear approximations and under the assumption that the dipole anisotropy domi-

nates the distortion, this can be written as [69]

$$y = \frac{7}{10} \int_0^{z_{re}} dz \frac{d\tau}{dz} \beta(z)^2, \quad (34)$$

where τ is the optical depth, $\beta(z)$ is the dipole temperature anisotropy in the CMB observed at redshift z , and the integral is taken up to the redshift of reionization z_{re} .

The FIRAS instrument on COBE provides an upper bound $y < 1.5 \times 10^{-5}$ (at 2σ) [113]. While this can constrain some void profiles, voids lacking an overdense outer shell are found not to be in tension with this upper bound [69]. The Gaussian void profile that we consider does not have a prominent overdense outer shell. Since we do not expect an interesting constraint, we chose not to evaluate the y -distortion, which would be uncertain in any case since the exact reionization history (and thus z_{re}) of the void model is unknown.

Another direct test of a local void is via the kinetic Sunyaev-Zel'dovich effect [114]. This has been applied to cluster kSZ observations (*e.g.*, Ref.[63, 115]) and to full-sky data [116] from the Atacama Cosmology Telescope (ACT) [117], and is found to place constraints on large voids. Allowing an inhomogeneous bang-time or correctly accounting for the effects of radiation (see [104, 105]) may potentially weaken these constraints while preserving the fits described here. Such an analysis is beyond the scope of the current paper but will be investigated in the future.

In summary, in this paper we have presented a local void model which fits SNe Ia and CMB data, local H_0 values, nucleosynthesis constraints and BAO *without* requiring dark energy and thus provides a counterexample to the claim that dark energy is necessary to fit these observations.

VIII. ACKNOWLEDGEMENTS

We would like to thank Shaun Hotchkiss, Timothy Clifton, Pedro Ferreira, Joe Zuntz and Jim Zibin for helpful discussions and correspondence, and Paul Hunt for his early involvement with this paper. SN is supported by an ORS award and a Clarendon Domus A scholarship from the University of Oxford and Merton College, Oxford.

-
- [1] G. R. Blumenthal, S. M. Faber, J. R. Primack and M. J. Rees, *Nature* **311**, 517 (1984).
 - [2] M. Davis, G. Efstathiou, C. S. Frenk and S. D. M. White, *Astrophys. J.* **292**, 371 (1985).
 - [3] G. Efstathiou, W. J. Sutherland and S. J. Maddox, *Nature* **348**, 705 (1990).
 - [4] G. F. Smoot *et al.*, *Astrophys. J.* **396**, L1 (1992).
 - [5] S. D. M. White, G. Efstathiou and C. S. Frenk, *Mon. Not. Roy. Astron. Soc.* **262**, 1023 (1993).

- [6] A. G. Riess *et al.* [Supernova Search Team Collaboration], *Astron. J.* **116**, 1009 (1998).
- [7] S. Perlmutter *et al.* [Supernova Cosmology Project Collaboration], *Astrophys. J.* **517**, 565 (1999).
- [8] G. Efstathiou *et al.* [2dFGRS Collaboration], *Mon. Not. Roy. Astron. Soc.* **330**, L29 (2002).
- [9] D. N. Spergel *et al.* [WMAP Collaboration], *Astrophys. J. Suppl.* **148**, 175 (2003).
- [10] D. J. Eisenstein *et al.* [SDSS Collaboration], *Astrophys. J.* **633**, 560 (2005).

- [11] C. R. Contaldi, H. Hoekstra and A. Lewis, *Phys. Rev. Lett.* **90**, 221303 (2003).
- [12] A. G. Riess *et al.* [Supernova Search Team Collaboration], *Astrophys. J.* **607**, 665 (2004).
- [13] P. Astier *et al.* [The SNLS Collaboration], *Astron. Astrophys.* **447**, 31 (2006).
- [14] W. M. Wood-Vasey *et al.*, *Astrophys. J.* **L666**, 694 (2007).
- [15] D. N. Spergel *et al.* [WMAP Collaboration], *Astrophys. J. Suppl.* **170**, 377 (2007).
- [16] S. Weinberg, *Rev. Mod. Phys.* **61**, 1 (1989).
- [17] P. Hunt and S. Sarkar, *Phys. Rev. D* **76**, 123504 (2007).
- [18] P. Hunt and S. Sarkar, *Mon. Not. Roy. Astron. Soc.* **401**, 547 (2010).
- [19] A. Blanchard, M. Douspis, M. Rowan-Robinson and S. Sarkar, *Astron. Astrophys.* **412**, 35 (2003).
- [20] S. Sarkar, *Gen. Rel. Grav.* **40**, 269 (2008).
- [21] T. Buchert, *Gen. Rel. Grav.* **32**, 105 (2000).
- [22] C. Wetterich, *Phys. Rev. D* **67**, 043513 (2003).
- [23] A. Ishibashi and R. M. Wald, *Class. Quant. Grav.* **23**, 235 (2006).
- [24] R. A. Vanderveld, E. E. Flanagan and I. Wasserman, *Phys. Rev. D* **76**, 083504 (2007).
- [25] D. L. Wiltshire, *Phys. Rev. Lett.* **99**, 251101 (2007).
- [26] B. M. Leith, S. C. C. Ng and D. L. Wiltshire, *Astrophys. J.* **672**, L91 (2008).
- [27] S. Khosravi, E. Kourkchi and R. Mansouri, *IJMP D18*, 1177 (2009).
- [28] J. Behrend, I. A. Brown and G. Robbers, *JCAP* **0801**, 013 (2008).
- [29] S. Rasanen, *JCAP* **0804**, 026 (2008).
- [30] N. Li, M. Seikel and D. J. Schwarz, *Fortsch. Phys.* **56**, 465 (2008).
- [31] A. Paranjape and T. P. Singh, *Phys. Rev. Lett.* **101**, 181101 (2008).
- [32] T. Biswas and A. Notari, *JCAP* **0806**, 021 (2008).
- [33] N. Brouzakis, N. Tetradis and E. Tzavara, *JCAP* **0804**, 008 (2008).
- [34] N. Brouzakis and N. Tetradis, *Phys. Lett. B* **665**, 344 (2008).
- [35] W. Valkenburg, *JCAP* **0906**, 010 (2009).
- [36] V. Marra, E. W. Kolb, S. Matarrese and A. Riotto, *Phys. Rev. D* **76**, 123004 (2007).
- [37] V. Marra, E. W. Kolb and S. Matarrese, *Phys. Rev. D* **77**, 023003 (2008).
- [38] K. Kainulainen and V. Marra, *Phys. Rev. D* **80**, 127301 (2009).
- [39] T. Mattsson, *Gen. Rel. Grav.* **42**, 567 (2010).
- [40] J. W. Moffat and D. C. Tatarski, *Astrophys. J.* **453**, 17 (1995).
- [41] K. Tomita, *Astrophys. J.* **529**, 26 (2000).
- [42] M. N. Celerier, *Astron. Astrophys.* **353**, 63 (2000).
- [43] K. Tomita, *Astrophys. J.* **529**, 38 (2000).
- [44] K. Tomita, *Prog. Theor. Phys.* **105**, 419 (2001).
- [45] K. Tomita, *Mon. Not. Roy. Astron. Soc.* **326**, 287 (2001).
- [46] K. Tomita, *Prog. Theor. Phys.* **106**, 929 (2001).
- [47] H. Iguchi, T. Nakamura and K. i. Nakao, *Prog. Theor. Phys.* **108**, 809 (2002).
- [48] K. Tomita, *Astrophys. J.* **584**, 580 (2003).
- [49] J. W. Moffat, *JCAP* **0510**, 012 (2005).
- [50] J. W. Moffat, *JCAP* **0605**, 001 (2006).
- [51] H. Alnes, M. Amarzguoui and O. Gron, *Phys. Rev. D* **73**, 083519 (2006).
- [52] R. Mansouri, arXiv:astro-ph/0512605.
- [53] R. A. Vanderveld, E. E. Flanagan and I. Wasserman, *Phys. Rev. D* **74**, 023506 (2006).
- [54] D. Garfinkle, *Class. Quant. Grav.* **23**, 4811 (2006).
- [55] D. J. H. Chung and A. E. Romano, *Phys. Rev. D* **74**, 103507 (2006).
- [56] T. Biswas, R. Mansouri and A. Notari, *JCAP* **0712**, 017 (2007).
- [57] H. Alnes and M. Amarzguoui, *Phys. Rev. D* **75**, 023506 (2007).
- [58] R. R. Caldwell and A. Stebbins, *Phys. Rev. Lett.* **100**, 191302 (2008).
- [59] S. Alexander, T. Biswas, A. Notari and D. Vaid, *JCAP* **0909**, 025 (2009).
- [60] C. Clarkson, B. Bassett and T. C. Lu, *Phys. Rev. Lett.* **101**, 011301 (2008).
- [61] J. P. Uzan, C. Clarkson and G. F. R. Ellis, *Phys. Rev. Lett.* **100**, 191303 (2008).
- [62] J. Garcia-Bellido and T. Haugboelle, *JCAP* **0804**, 003 (2008).
- [63] J. Garcia-Bellido and T. Haugboelle, *JCAP* **0809**, 016 (2008).
- [64] T. Clifton, P. G. Ferreira and K. Land, *Phys. Rev. Lett.* **101**, 131302 (2008).
- [65] K. Bolejko and J. S. B. Wyithe, *JCAP* **0902**, 020 (2009).
- [66] A. Blanchard, M. Douspis, M. Rowan-Robinson and S. Sarkar, *Astron. Astrophys.* **449**, 925 (2006).
- [67] T. Clifton, P. G. Ferreira and J. Zuntz, *JCAP* **0907**, 029 (2009).
- [68] J. P. Zibin, A. Moss and D. Scott, *Phys. Rev. Lett.* **101**, 251303 (2008).
- [69] A. Moss, J. P. Zibin and D. Scott, arXiv:1007.3725 [astro-ph.CO].
- [70] T. Biswas, A. Notari, W. Valkenburg, *JCAP* **1011**, 030 (2010). [arXiv:1007.3065 [astro-ph.CO]].
- [71] K. Enqvist, T. Mattsson, *JCAP* **0702**, 019 (2007). [astro-ph/0609120].
- [72] J. P. Zibin, *Phys. Rev. D* **78**, 043504 (2008).
- [73] E. Komatsu *et al.* [WMAP Collaboration], *Astrophys. J. Suppl.* **192**, 18 (2011). [arXiv:1001.4538 [astro-ph.CO]].
- [74] J. Martin and C. Ringeval, *Phys. Rev. D* **69**, 083515 (2004); *Phys. Rev. D* **69**, 127303 (2004).
- [75] N. Kogo, M. Sasaki and J. Yokoyama, *Phys. Rev. D* **70**, 103001 (2004).
- [76] N. Kogo, M. Sasaki and J. Yokoyama, *Prog. Theor. Phys.* **114**, 555 (2005).
- [77] A. Shafieloo, T. Souradeep, P. Manimaran, P. K. Panigrahi and R. Rangarajan, *Phys. Rev. D* **75**, 123502 (2007).
- [78] A. Shafieloo and T. Souradeep, *Phys. Rev. D* **70**, 043523 (2004) [arXiv:astro-ph/0312174].
- [79] D. Tocchini-Valentini, Y. Hoffman and J. Silk, *Mon. Not. Roy. Astron. Soc.* **367**, 1095 (2006) [arXiv:astro-ph/0509478].
- [80] D. Tocchini-Valentini, M. Douspis and J. Silk, *Mon. Not. Roy. Astron. Soc.* **359**, 31 (2005).
- [81] G. Nicholson, C. R. Contaldi and P. Paykari, *JCAP* **1001**, 016 (2010).
- [82] G. Nicholson and C. R. Contaldi, *JCAP* **0907**, 011 (2009).
- [83] K. Ichiki and R. Nagata, *Phys. Rev. D* **80**, 083002 (2009).
- [84] J. A. Adams, G. G. Ross and S. Sarkar, *Nucl. Phys. B* **503**, 405 (1997).

- [85] T. Gherghetta, C. F. Kolda and S. P. Martin, Nucl. Phys. B **468**, 37 (1996).
- [86] P. Hunt and S. Sarkar, Phys. Rev. D **70**, 103518 (2004).
- [87] J. A. Adams, B. Cresswell and R. Easther, Phys. Rev. D **64**, 123514 (2001).
- [88] H. V. Peiris *et al.* [WMAP Collaboration], Astrophys. J. Suppl. **148**, 213 (2003).
- [89] L. Covi, J. Hamann, A. Melchiorri, A. Slosar and I. Sorbera, Phys. Rev. D **74**, 083509 (2006).
- [90] J. Hamann, L. Covi, A. Melchiorri and A. Slosar, Phys. Rev. D **76**, 023503 (2007).
- [91] S. Hotchkiss and S. Sarkar, JCAP **1005**, 024 (2010).
- [92] P. Brax and E. Cluzel, arXiv:1010.4462 [hep-th].
- [93] M. Hicken *et al.*, Astrophys. J. **700**, 1097 (2009).
- [94] R. Amanullah *et al.*, Astrophys. J. **716**, 712 (2010).
- [95] W. L. Freedman *et al.* [HST Collaboration], Astrophys. J. **553**, 47 (2001).
- [96] K. Nakamura *et al.* [Particle Data Group (see review by B. Fields and S. Sarkar)], J. Phys. G **37**, 075021(2010).
- [97] W. J. Percival *et al.*, Mon. Not. Roy. Astron. Soc. **401**, 2148 (2010).
- [98] J. Guy *et al.*, arXiv:1010.4743 [astro-ph.CO].
- [99] A. Lewis, A. Challinor and A. Lasenby, Astrophys. J. **538**, 473 (2000).
- [100] D. J. Fixsen, Astrophys. J. **707**, 916 (2009).
- [101] W. L. Freedman and B. F. Madore, Annu. Rev. Astron. Astrophys. **48**, 673 (2010)
- [102] G. A. Tammann, A. Sandage and B. Reindl, Astrophys. J. **679**, 52 (2008).
- [103] A. G. Riess *et al.*, Astrophys. J. **699**, 539 (2009).
- [104] M. Regis and C. Clarkson, arXiv:1003.1043 [astro-ph.CO].
- [105] C. Clarkson and M. Regis, arXiv:1007.3443 [astro-ph.CO].
- [106] S. February, J. Larena, M. Smith and C. Clarkson, Mon. Not. Roy. Astron. Soc. **405**, 2231 (2010).
- [107] D. J. Eisenstein and W. Hu, Astrophys. J. **496**, 605 (1998).
- [108] E. Gaztanaga, R. Miquel and E. Sanchez, Phys. Rev. Lett. **103**, 091302 (2009).
- [109] E. Gaztanaga, A. Cabre and L. Hui, Mon. Not. Roy. Astron. Soc. **399**, 1663 (2009).
- [110] J. Miralda-Escude, arXiv:0901.1219 [astro-ph].
- [111] E. A. Kazin, M. R. Blanton, R. Scoccimarro, C. K. McBride and A. A. Berlind, Astrophys. J. **719**, 1032 (2010).
- [112] A. Lewis and S. Bridle, Phys. Rev. D **66**, 103511 (2002).
- [113] D. J. Fixsen, E. S. Cheng, J. M. Gales, J. C. Mather, R. A. Shafer and E. L. Wright, Astrophys. J. **473**, 576 (1996).
- [114] R. A. Sunyaev and Y. B. Zeldovich, Comments Astrophys. Space Phys. **4**, 173 (1972); R. A. Sunyaev and Y. B. Zeldovich, Mon. Not. Roy. Astron. Soc. **190**, 413 (1980).
- [115] C. M. Yoo, K. i. Nakao and M. Sasaki, JCAP **1010**, 011 (2010) [arXiv:1008.0469 [astro-ph.CO]].
- [116] P. Zhang and A. Stebbins, arXiv:1009.3967 [astro-ph.CO].
- [117] S. Das *et al.*, arXiv:1009.0847 [astro-ph.CO]; J. Dunkley *et al.*, arXiv:1009.0866 [astro-ph.CO].